Endocrine (2017) 58:153–166
DOI 10.1007/s12020-017-1393-3

ORIGINAL ARTICLE

The roles of microRNA-34b-5p in angiogenesis of thyroid carcinoma

Hamidreza Maroof[1] · Farhadul Islam[1,2] · Armin Ariana[1] · Vinod Gopalan[1] · Alfred K. Lam[1]

Received: 3 June 2017 / Accepted: 9 August 2017 / Published online: 24 August 2017
© Springer Science+Business Media, LLC 2017

Abstract
Purpose This study aims to determine the expression of miR-34b-5p in thyroid carcinomas and to investigate the role of miR34b-5p in the modulation of proteins involved in angiogenesis of thyroid carcinoma cells.
Methods The expressions of miR-34b-5p levels in five cell lines and 65 tissue samples from thyroid carcinomas were examined by real-time polymerase chain reaction. An exogenous miR-34b-5p (mimic) transiently overexpress miR-34b-5p in theses thyroid carcinoma cells. The effects of miR-34b-5p overexpression on the proteins involved in angiogenesis and cell cycle regulations (VEGF-A, Bcl-2 and Notch1) were investigated by Western blot, immunofluorescence, enzyme-linked immunosorbent assay followed by cell cycle analysis and apoptosis assays.
Results miR-34b-5p is markedly downregulated in all thyroid carcinoma cell lines and tissues samples when compared with non-neoplastic immortalised thyroid cell line and non-neoplastic thyroid tissues, respectively. The expression levels of miR-34b were significantly associated with T-stages of thyroid carcinomas ($p = 0.042$). Downregulation of VEGF-A, Bcl-2 and Notch1 proteins in thyroid carcinoma cells were noted in cells that transiently transfected with miR-34b-5p mimic. In addition, enzyme-linked immunosorbent assay confirmed the decreased expression of VEGF in thyroid carcinoma cells after transfection with miR-34b-5p mimic. Furthermore, miR-34b-5p mimic transfection induces significant accumulation of cells in G0-G1 of the cell cycle by blocking of their entry into the S transitional phase as well as increasing the total apoptosis.
Conclusions miR-34b-5p functions as a potent regulator of angiogenesis, apoptosis and cell proliferation via modulation of VEGF-A, Bcl-2 and Notch1 proteins. It could be a target for developing treatment strategies of thyroid carcinoma with aggressive clinical behaviour.

Keywords Thyroid carcinoma · miR-34b · Angiogenesis · VEGF · Bcl-2 · Notch1

Introduction

Papillary thyroid carcinoma is the most common thyroid cancer, and patients with cancer have relatively good prognosis [1]. In some instances, papillary thyroid carcinoma could progress to an aggressive type of thyroid cancer, anaplastic thyroid carcinoma [2].

Angiogenesis is an essential process for growth and metastases of cancer mediated by vascular endothelial growth factor (VEGF) [3, 4]. Thyroid carcinomas are good models to study angiogenesis of cancer as they are vascular [1]. Angiogenesis has substantial clinical impacts in the pathogenesis and progression of thyroid cancer mediated by VEGF [5–7]. Angiogenesis is activated in the hypoxic

Electronic supplementary material The online version of this article (doi:10.1007/s12020-017-1393-3) contains supplementary material, which is available to authorized users.

✉ Alfred K. Lam
a.lam@griffith.edu.au

[1] Cancer Molecular Pathology, School of Medicine and Menzies Health Institute Queensland, Griffith University, Gold Coast, QLD 4222, Australia

[2] Department of Biochemistry and Molecular Biology, University of Rajshahi, Rajshahi 6205, Bangladesh

microenvironment of cancer [8]. This angiogenic switch directly leads to the secretion of angiogenic factors such as VEGF and indirectly activates proliferating genes, such as *B-cell lymphoma 2* (*Bcl-2*) and *Notch homolog 1* (*Notch1*) [9–11].

VEGF-A has been identified to play a significant role as a proangiogenic factor involved in thyroid cancer [12]. Therapies targeting the VEGF have become a promising tool in some cancers, such as lung and colorectal cancers [13]. However, many cancers are resistant to these therapies [13–18]. Therefore, recognition of new angiogenesis regulators could improve the effectiveness of these therapeutic strategies.

The mature *miR-34* family is a part of the *p53* tumour suppressor network [19, 20]. In thyroid cancer, Yip and colleagues have shown the role of miR-34b in predicting the aggressiveness of papillary thyroid carcinoma [21]. Also, negative expression of VEGF, Notch1 and Bcl-2 proteins correlated with the presence of miR-34b-5p [22–26]. Furthermore, these studies showed that the 3′ UTR of VEGF, Notch1 and Bcl-2 mRNA contain miR-34b-5p binding site and they can be regulated by miR-34b-5p [22–26].

There is no previous study on the role of miR-34b on VEGF, Notch1 and Bcl-2 in thyroid carcinoma. Thus, the aim of this study is to determine the function of miR-34b-5p in the pathogenesis of thyroid carcinoma. Furthermore, this study also investigated the role of miR34b-5p in the modulation of angiogenesis initiation process by examining the expression of VEGF-A, Bcl-2 and Notch1 in thyroid carcinoma cells.

Materials and methods

Human tissue samples

We have collected cancer tissue from 65 patients operated for papillary thyroid carcinoma. Ethics approval for the use of human tissue samples was obtained from Griffith University (MED/19/08/HREC). Seven non-neoplastic thyroid tissues from patients diagnosed with nodular hyperplasia of thyroid were used as controls in this study (Supplementary fig. S1).

Cell culture

Five thyroid carcinoma cell lines were used in this study. Four of the cancer cell lines were purchased from the Deutsche Sammlung von Mikroorganismen und Zellkulturen GmBH-German Collection of microorganisms and cell cultures (DSMZ, Braunschweig, Germany). They were B-CPAP (from metastasizing human papillary thyroid carcinoma), 8505C (from metastatic human anaplastic thyroid carcinomas in a lymph node with primary papillary thyroid carcinoma), MB-1(from anaplastic thyroid carcinoma) and BHT-101 (from metastatic anaplastic thyroid carcinoma in the lymph node). The remaining cancer cell line was a human papillary thyroid carcinoma cell line (K1) which was obtained from European Collection of Cell Cultures (ECACC). A non-neoplastic thyroid follicular cell line (Nthy-ori 3-1, from ECACC) was used as a control. The cell lines were authenticated in the standard protocol (using multiplex polymerase chain reaction of mini-satellite markers for DNA fingerprinting and identification of short tandem repeats of cell lines and cytogenetics), and the passage number of these cell lines was less than nine. All the cell lines were maintained according to the suppliers and were cultured in a humidified incubator in an atmosphere of 5% CO_2 and 95% air at 37 °C

Quantification of miR-34b-5p expression

The miR-34b-5p expression level was quantified by real-time quantitative polymerase chain reaction (qRT-PCR) using Hs_miR-34b*_2 miScript Primer Assay (Qiagen, Venlo, Limburg, Netherlands) following the suggested protocol. Samples were normalised using the housekeeping gene RNU6B RNA (Hs_ RNU6B_2 miScript Primer Assay, Qiagen). Total RNA from cells and tissue samples was extracted using NucleoSpin® miRNA Kit (MACHEREY-NAGEL, Duren, Germany) and Qiagen miRNeasy FFPE Kits (Qiagen Pty. Ltd., Hilden, NRW, Germany), respectively, with a DNase supplementary step. Then, cDNA was synthesised using miScript II RT Kit (Qiagen) according to the manufacturer instructions. Amplification, detection and analysis were performed with an IQ5 multicolour Real-Time PCR detection system (BIO-RAD, Hercules, CA, USA).

Real-time PCR amplifications were performed in a 20 µl reaction volume consisting of 10 µl QuantiTect SYBR Green PCR Master Mix (Qiagen), 1 µl miScript Primer Assay (Qiagen), 1 µl of miScript Universal Primer (Qiagen), and 5 µl of cDNA template at 2 ng/µl stock and 3 µl RNase- free water. All qRT-PCR reactions were carried out in triplicates with non-template controls as previously published protocol [27]. Expression of miR-34b-5p was presented as the ratio between miR-34b-5p and RNU6b. The $2^{-\Delta\Delta ct}$ method was used to calculate the fold changes of miRNA in each sample group. Less than 0.5-fold changes were considered as low expression. Fold changes between 0.5 and 2 were considered as normal expression whereas fold changes of more than two were considered as high expression.

miR-34 mimics transfection

Exogenous miR-34b-5p (mimic) (Syn-hsa-miR-34b-5p) and HiPerFect transfection reagent were purchased from Qiagen. Mature miR-34b mimic sequence (guide strand) was 5′ UAGGCAGUGUCAUUAGCUGAUUG-3′. Transfection was performed according to our previously published protocol [28, 29]. Briefly, thyroid cancer cells were transfected immediately after being seeded at a density of 25×10^4 cells/well in six-well plate with miR-34b-5p mimics and with a non-targeting control, positive control (miR-1; miR-1 is only expressed in muscle cells and is not expressed in other cell types. As hsa-miR-1 is not expressed in thyroid cell lines used in this study, then transfection of this mimic and subsequent analysis of its target can be used as a positive control experiment) and negative control siRNA (scramble control) (Qiagen), using the HiperFect transfection reagent (Qiagen) for overexpression of miR-34b-5p. A final concentration of 5 nM, as well as 48-h incubation period, was selected for both transfections.

Immunofluorescence

In the immunofluorescence analysis, the cells were transfected as described above after being cultivated on a glass culture slide (BD Biosciences, San Jose, CA, USA). The cells were fixed in 4% cold paraformaldehyde/phosphate buffer saline (PBS) for 25 min, permeabilised in 0.4% triton X-100 for 8 min. They were blocked in 5% normal goat serum/PBS (Sigma–Aldrich, St. Louis, MO, USA) for 45 min. Then, they were incubated with antibodies against Bcl-2 (N-19, 1:200; Santa Cruz Biotechnology, Dallas, TX, USA), VEGF-A (A-20, 1:200 dilution; Santa Cruz Biotechnology), Notch1 (H-131, 1:300 dilution; Santa Cruz Biotechnology) overnight at 4 °C. Afterwards, the cells were incubated with Texas Red-labelled secondary antibody (1:1000 dilution; Life technologies, St. Louis, MO, USA) for 1 h at room temperature. As a negative control, all staining was performed without the primary antibody. After being counterstained with 4′,6-diamidino-2-phenylindole (Sigma–Aldrich), confocal laser scanning microscopic images were captured with an Eclipse Ti-E microscope (Nikon Instruments, Inc., Melville, NY, USA) using a plan apochromat 60×/1.40 objective and NIS-Elements imaging software platform (Nikon).

Western blot analysis and antibodies

After transfection, the cells were lysed in Cell Lysis Buffer NP40 (50 mM Tris, pH 7.4, 250 mM NaCl, 5 mM EDTA, 50 mM NaF, 1 mM Na3VO4, 1% Nonidet P40 and 0.02% NaN3) (Invitrogen Carlsbad, CA, USA) supplemented with protease inhibitor cocktail (Sigma-Aldrich), phenylmethanesulfonyl fluoride solution (Sigma) and phosphatase inhibitor cocktail (Cell Signaling, Danvers, MA, USA). Then, protein lysates were prepared, and protein concentration was quantified using the Macherey-Nagel protein assay kit (MACHEREY-NAGEL GmbH & Co.KG, Düren, Germany).

Equal quantities of 20 µg protein samples were loaded on 4–15% precast polyacrylamide gel (Mini-PROTEAN TGX Precast Gel, Bio-Rad) and were transferred onto polyvinylidene-difluoride membranes (Trans-Blot Turbo Mini PVDF Transfer Packs, Bio-Rad) using the blotting instrument (Trans-Blot Turbo Transfer Starter System, Bio-Rad). Blocking was performed with 5% non-fat milk in TBST (Tris buffered saline-Tween 20: 120 mmol/l Tris–HCl, pH 7.4, 150 mmol/l NaCl, and 0.05% Tween 20) for 1 h at room temperature. The membrane was incubated with anti-Bcl-2 (Sc-492), 1:500 dilution; anti-VEGF-A (Sc-152), 1:200 dilution; anti-Notch1 (Sc-9170), 1:200 dilution and anti-ß-actin (Sc-4778), 1:1000 dilution (Santa Cruz Biotechnology) overnight at 4˚C. Following the manufacturer's protocol, blots were washed six times with TBST, incubated for one and half hour with horseradish peroxidase-conjugated secondary antibody (1:5000 dilution) (Santa Cruz Biotechnology) at room temperature. The blots were then developed and visualised as previously published protocol [30]

Enzyme-linked immunosorbent (ELISA) assay

Cells transfected with miR-34b-5p mimic were cultured at a density of 2×10^5 cells/well in six-well plates. After 48 h, the media was collected and quantified for secreted VEGF using a Human VEGF ELISA kit (Life technologies, St. Louis, MO, USA), according to the manufacturer's instructions.

Cell cycle analysis

After 48 h transfection, cells were harvested by trypsinization and centrifugation at 1500 rpm for 5 min. Then, the supernatant media was discarded. After that, the cells were washed with ice-cold PBS and fixed in 70% ice-cold ethanol at −20 °C for 1 h. Subsequently the cells were centrifuged again at 1500 rpm for 5 min and were washed twice with PBS. These cells were then stained with propidium iodide (PI) (50 mg/ml in PBS), RNase (50 mg/ml) and Triton X-100 (0.1%) and incubated for 40 min at 37 °C and analysed using a FACS Calibur flow cytometer (BD Biosciences). Data were analysed to calculate the percentage of the cell population in each phase using the FlowJo single-cell analysis software (FLOWJO, LLC, Ashland, OR, USA).

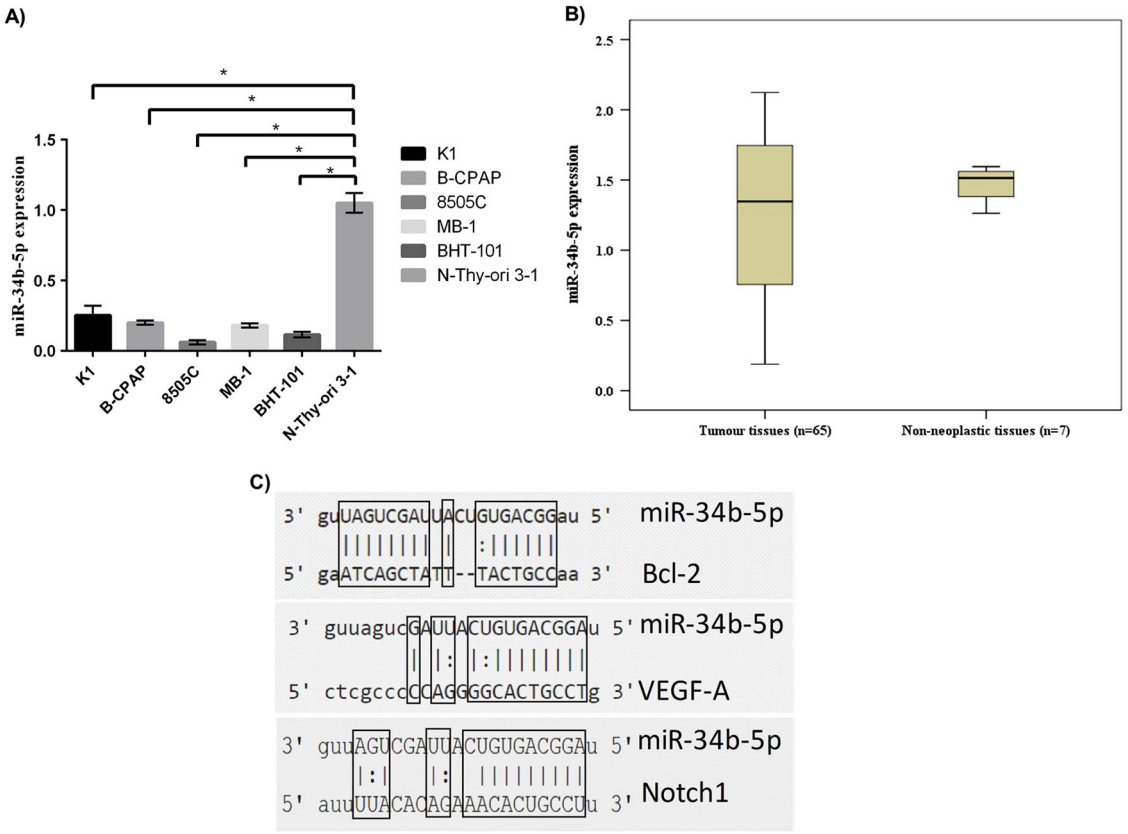

Fig. 1 Expression in thyroid cancer cells and tissues of miR-34b-5p and targets interaction sites. **a** Expression of miR-34b in thyroid carcinoma: The miR-34b-5p decreased significantly in all thyroid carcinomas ($p < 0.05$). miR-34b-5p expression was lower in 8505C (anaplastic thyroid carcinoma from a papillary thyroid carcinoma origin) and BHT-101 (anaplastic thyroid carcinoma metastases in lymph node) than K1 (papillary thyroid carcinoma), B-CPAP (metastasizing papillary thyroid carcinoma) and MB-1(anaplastic thyroid carcinoma) when compared with the Nthy-ori 3-1 (non-neoplastic thyroid follicular cell line) ($p < 0.05$). RNU6B was used to normalize the mRNA level. An asterisk indicates $p < 0.05$, when compared to Nthy-ori-3-1. The quantitative values were expressed as means ± SD of triplicate measurements. They are representative of three separate experiments. **b** Expression of miR-34b-5p in cancer and non-neoplastic thyroid tissue samples after normalization with internal control RNU-6B. Bar represent the standard deviation of the values in each group. **c** Alignment of *Bcl-2*, *Notch1* and *VEGF-A* with the miR-34b-5p: The transcript is positioned and matched with miR-34b-5p between 190–210, 166–184 and 845–867 base pairs of *Bcl-2*, *Notch1* and *VEGF-A* respectively. microRNA.org predicated mirSVR of −0.2530, −1.357 and −0.1480 for *Bcl-2*, *Notch1* and *VEGF-A* respectively (http://www.microrna.org/). Genes that have a score of −1.0 or lower, corresponding to the top 7% of predictions, have more than a 35% probability of having a (*Z*-transformed) log expression change of at least −1 (downregulation by at least a standard deviation in terms of log expression changes) and better than 50% probability of a log expression change of at least −0.5. Thus, mirSVR scores can be converted to a probability of downregulation. This can be used as a guide for selecting a meaningful cut-off for reporting target sites. (Betel et al. 2010) [53]

Apoptosis assay

A membrane permeability/Dead Cell Apoptosis Kit (Invitrogen) was used to measure the apoptotic cell. Briefly, after 48 h of transient transfection, cells were trypsinized, washed twice with ice-cold PBS and resuspended in PBS at a concentration of 25×10^4/ml cells in a total volume of 1 ml. After that, 1 µl of YO-PRO®−1 and 1 µl of PI were added. All the samples were kept in the dark for 20 min at room temperature. Finally, the numbers of apoptotic cells were analysed using a FACS Calibur flow cytometer (BD Biosciences, San Jose, CA, USA) and calculated with FlowJo single-cell analysis software (FLOWJO, LLC, Ashland, OR, USA).

Data analysis

Results were analysed using GraphPad Prism 7.0 (Graph Pad Software, SanDiego, CA, USA) and were expressed as means ± SD (standard deviation). All of the in vitro experiments were performed at least three times. Statistical comparisons between groups were conducted using one-way ANOVA. A p value of < 0.05 was considered statistically significant and individual p-value was shown in the figures.

Results

miR-34b expression is altered in human thyroid carcinoma tissues and cell lines

To investigate changes in the miR-34b-5p expression level in human thyroid carcinomas, we examined a series of human thyroid carcinoma tissues, cell lines (K1, B-CPAP, 8505C, MB-1, BHT-101) and a non-neoplastic immortalised thyroid cell line (Nthy-ori3-1). miR-34b-5p showed significant downregulation in thyroid carcinoma cells when compared to the Nthy-ori-3-1cell line ($p < 0.05$). The lowest level of miR-34b-5p was noted in carcinoma cell lines derived from more aggressive thyroid carcinoma–anaplastic thyroid carcinoma (8505C, MB-1 and BHT-101) (Fig. 1a). Notable reduced expression of miR-34b-5p in cancer tissues was noted when compared to that of non-neoplastic thyroid tissue samples (Fig. 1b). The fold changes of miR-34b in thyroid cancer tissues samples was noted in the range of 0.000909 to 10.858 (0.487 ± 1.585).

On tissue level, 88% (57/65) of the patients with thyroid carcinoma had shown downregulation of miR-34b expression whereas 7% (5/65) of the patients showed high miR-34b expression (Table 1). Approximately 5% (3/65) of the patients with thyroid carcinoma exhibited no change in miR-34b expression when compared to non-neoplastic thyroid tissues. In addition, miR-34b downregulation was associated with T-stage of the thyroid carcinoma (Table 1). In thyroid carcinomas of advanced T stages (3 or 4), all had either low or normal expression whereas, in thyroid carcinomas of earlier T stages (1 or 2), 91.8% had either low or normal expression ($p = 0.042$).

Given that expression of miR-34b-5p was notably downregulated in thyroid carcinoma cell lines and tissues ($p < 0.05$), we chose to restore miR-34b-5p in thyroid carcinoma cell lines to study its various cellular and biological effects.

miR-34b-5p regulates markers of cell proliferation

As a potent target for miR-34b-5p, the expression of VEGF, Notch1 and Bcl-2 proteins can be suppressed due to their affinity to bind miR34b (Fig. 1c). To gain an insight into the mechanism by which miR-34b-5p inhibits Bcl-2 and Notch1, we identified the miR-34b-5p binding site in the Bcl-2 and Notch1 mRNA 3′ UTR region (Fig. 1c). Figure 1c reveals the sequence matches between miR-34b-5p and the *VEGF, Notch1* and *Bcl-2* genes.

After 48-h transfections, Western blot analysis showed that Bcl-2 and Notch1 protein expressions were markedly reduced in miR-34b-5p transfected cell lines when compared with miR-1 transfected and scramble control (Figs. 2 and 3) ($p < 0.05$).

Immunofluorescence analysis confirmed the Western blot results. After 48 h of transfection, the immunofluorescence analysis of the Bcl-2 and Notch1 revealed that miR-34b-5p overexpression potently suppresses Bcl-2 and Notch1 protein expression in 8505C (Fig. 4a) and BHT-101 (Fig. 4b) when compared with miR-1 transfected and

Table 1 Expression of miR-34b and its correlation with clinicopathological parameters of patients with thyroid cancer

Parameters	Total no.	High expression	Normal expression	Low expression	*p* values
miR-34b expression	65 (100%)	5 (7.7%)	3 (4.6%)	57 (87.7%)	–
Sex					
Male	19 (29.2%)	1 (5.3%)	0 (0%)	18 (94.7%)	0.249
Female	46 (70.8%)	4 (8.7%)	3 (6.5%)	39 (84.8%)	
Age					
<55 years	47 (72.3%)	2 (4.2%)	3 (6.4%)	42 (89.4%)	0.118
≥55 years	18 (27.7%)	3 (16.7%)	0 (0%)	15 (83.3%)	
Size					
<40 mm	50 (76.9%)	5 (10.0%)	2 (4.0%)	43 (86.0%)	0.240
≥40 mm	15 (23.1%)	0 (0%)	1 (6.7%)	14 (93.3%)	
T-stage					
T1 or T2	54 (83.1%)	5 (9.2%)	1 (1.9%)	48 (88.9%)	**0.042**
T3 or T4	11 (16.9%)	0 (0%)	2 (18.2%)	9 (81.8%)	
Lymph node invasion					
Positive	34 (52.3%)	3 (8.8%)	1 (2.9%)	30 (88.3%)	0.576
Negative	31 (47.7%)	2 (6.4%)	2 (6.5%)	27 (87.1%)	
Stage					
Stage 1	55 (84.6%)	4 (7.3%)	3 (5.4%)	48 (87.3%)	0.581
Stage 2	10 (15.4%)	1 (10.0%)	0 (0%)	9 (90.0%)	

bold values are significant *p* value

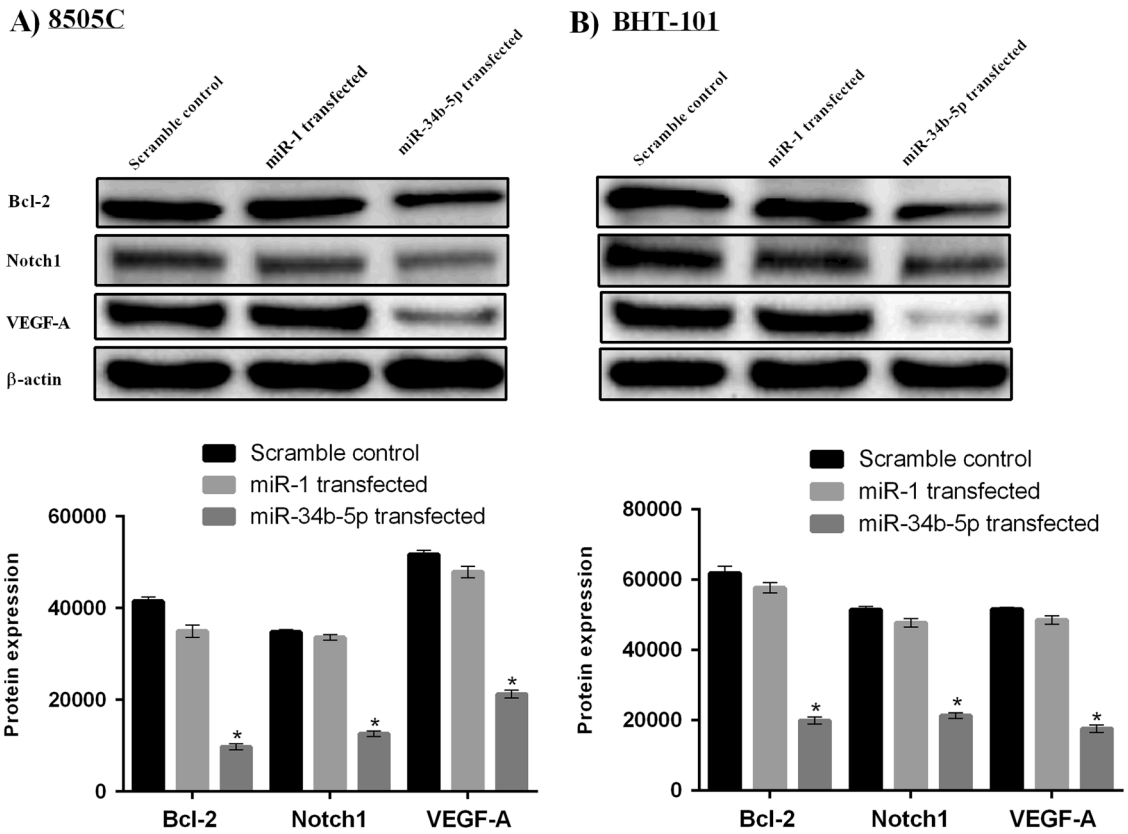

Fig. 2 miR-34b-5p decreased the expression of Bcl-2, Notch1 and VEGF-A in 8505C and BHT-101 detected by Western blotting. In 8505C (**a**) and BHT-101 (**b**) cells, expression of Bcl-2, Notch1 and VEGF-A were significantly reduced in the miR-34b-5p mimic transfected groups when compared to miR-1 transfected and scramble control groups. β-actin was used as a sample loading control; *y*-axis comparison diagrams shows Bcl-2, Notch1 and VEGF-A protein expressions based on signal absorption. Results were representative of three independent experiments. Results presented as mean ± SD; and asterisk implies as probability value $p < 0.05$ when compared to control (8505C: anaplastic thyroid carcinoma from a papillary thyroid carcinoma origin; BHT-101: metastatic anaplastic thyroid carcinoma in lymph node)

scramble control ($p < 0.05$). Fewer immunofluorescence distributions were noted in the nucleus and cytoplasm for Bcl-2 and in the cytoplasm for Notch1 when compared with miR-1 transfected and scramble control (supplementary fig. S2). This finding suggested that Bcl-2 and Notch1 are direct targets of miR-34b-5p, consistent with the data from the Western blot analysis.

miR-34b-5p downregulates endogenous VEGF-A expression as a hallmark of angiogenesis in thyroid cancer cell lines

To investigate the hypothesis that miR-34b-5p negatively regulate VEGF-A expression, the thyroid carcinoma cells were overexpressed with miR-34b-5p mimic (5 nM) for 48 h, and the VEGF-A protein level was determined afterwards. Western blot analysis showed a significant reduction in VEGF-A protein expression levels following miR-34b-5p overexpression when compared to miR-1 transfected and scramble control groups (Figs. 2, 3) ($p < 0.05$). Downregulation of VEGF-A by miR-34b-5p mimic in thyroid carcinoma has been confirmed by immunofluorescence analysis which showed decreased expression of VEGF-A protein. A remarkable reduction in the expression of VEGF-A protein was noted in the thyroid carcinoma cells in 8505C (Fig. 4a) and BHT-101 (Fig. 4b) when compared with miR-1 transfected and scramble controls ($p < 0.05$). Other thyroid carcinoma cells (K1, B-CPAP and MB-1) showed only slight changes in the expression of VEGF-A protein when compared with miR-1 transfected and scramble control (supplementary fig. S2).

Overexpression of miR-34b-5p inhibits VEGF expression in thyroid cancer cell lines supernatant

ELISA results showed that when compared with the non-neoplastic immortalised thyroid cell line, the expression of VEGF in supernatant fractions of the thyroid carcinoma

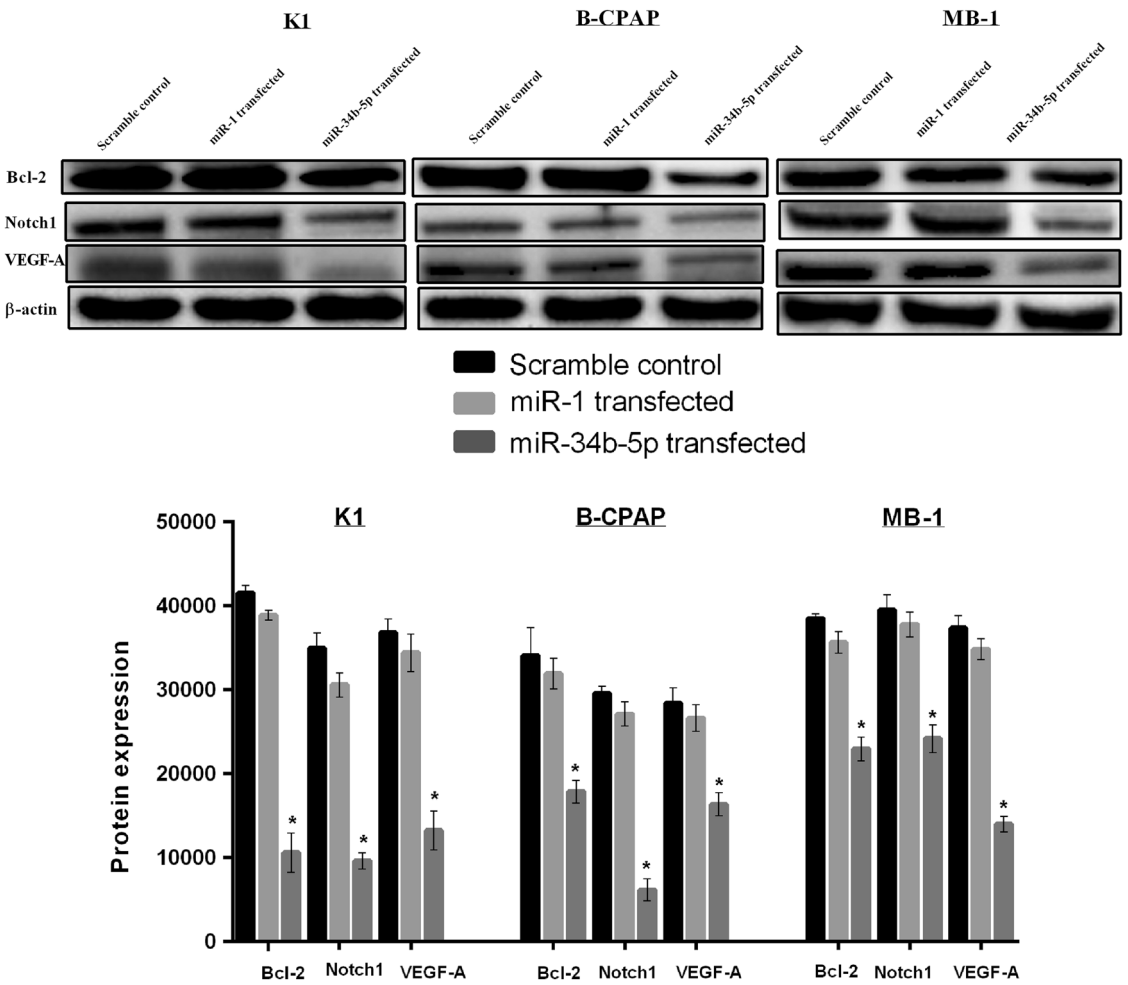

Fig. 3 miR-34b-5p is also involved in repressing Bcl-2, Notch1 and VEGF-A levels in K1, B-CPAP and MB-1 detected by Western blotting. After 48 h transfection with miR-34b-5p mimic, decreased pattern of Bcl-2, Notch1 and VEGF-A protein expressions were noted in K1, B-CPAP and MB-1 cells when miR-34b-5p mimic transfected group compared with miR-1 transfected and scramble control groups. β-actin was used as a sample loading control; *y*-axis comparison diagrams shows Bcl-2, Notch1 and VEGF-A protein expressions based on signal absorption. Results were representative of three independent experiments. Results presented as mean ± SD; and asterisk implies as probability value $p < 0.05$ when compared to control (K1: papillary thyroid carcinoma; B-CPAP: metastasizing papillary thyroid carcinoma; MB-1: anaplastic thyroid carcinoma)

cells (KI, B-CPAP, 8505C, MB-1 and BHT-101) transfected with miR-34b-5p was inhibited by 54, 72, 69, 58 and 45%, respectively (Fig. 4c) ($p < 0.05$). The above data revealed that overexpression of miR-34b-5p resulted in downregulation of Bcl-2, Notch1 and VEGF-A.

miR-34b-5p caused cell cycle arrest in thyroid cancer cells

The concentration of miR-34b-5p was raised to 15 nM. After 48 h of tranfection, the cells were studied by flow cytometry. Cell cycle arrest was observed at this time point. miR-34b-5p showed significant statistical differences in thyroid cancer cell cycle changes compared to miR-1(15 nM) and control groups ($p < 0.05$). Following miR-34b-5p overexpression, there was a significant increase in the accumulation of cells in G0-G1 phase as well as cell number reduced in the synthetic or S phase in all selected five thyroid cancer cell lines, especially in the thyroid carcinoma cells from B-CPAP and BHT-101 (Fig. 5) ($p < 0.05$).

In the K1 (papillary thyroid carcinoma) cells, mimic transfection of miR-34b-5p (15 nM) showed a significant arrest in the G0-G1 phase (11.36% ± 5.91) and a significant drop in S phase and G2/M phase after 48 h of transfections when compared with miR-1(15 nM)-transfected and scramble control groups ($p < 0.05$) (Fig. 5a). After 48 h of transfections, the percentage of cells in the G0-G1 phase in the B-CPAP (metastasizing papillary

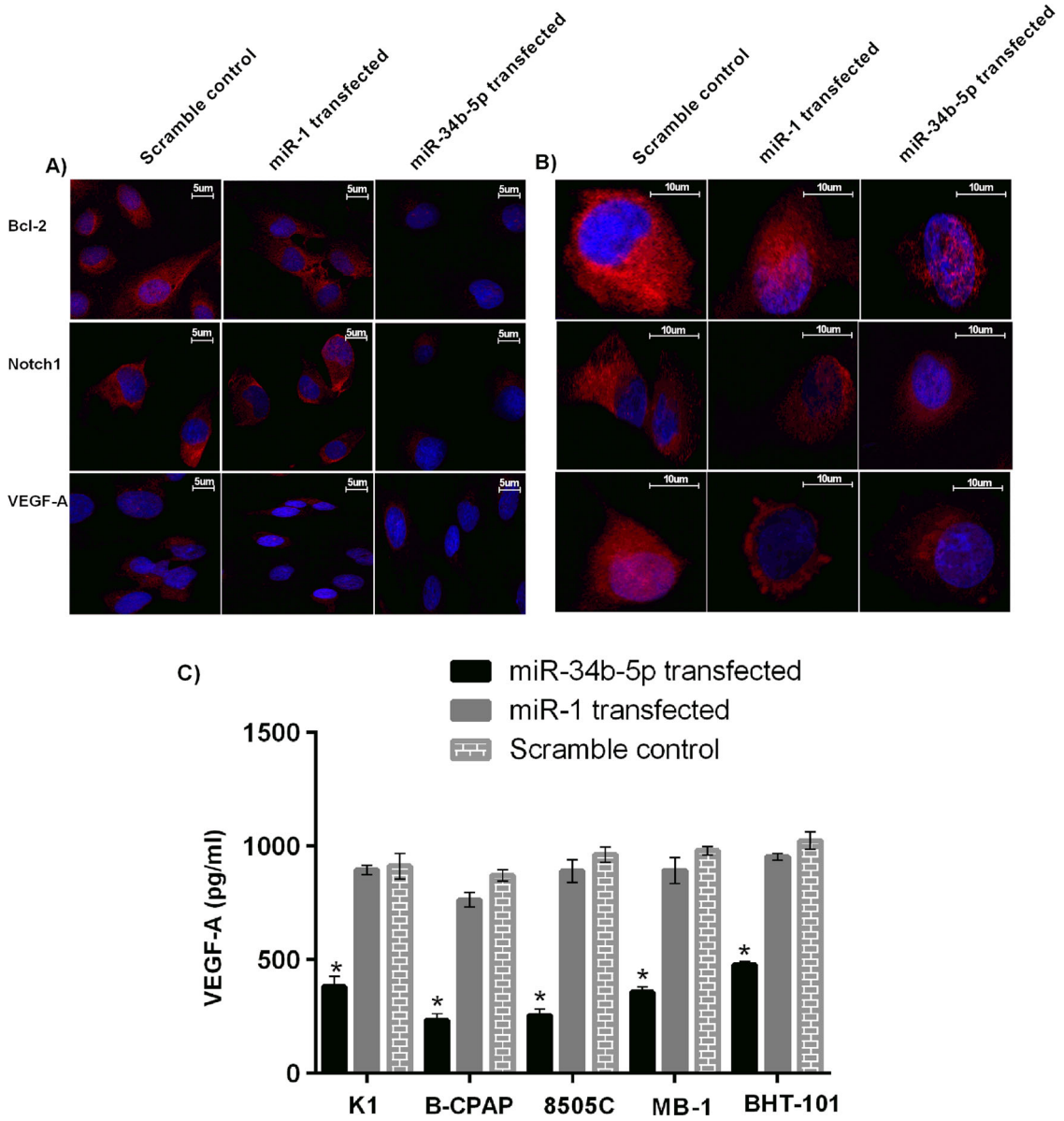

Fig. 4 Confirmation of miR-34b-5p-mediated alteration of targets proteins (Bcl-2, Notch1 and VEGF-A) in 8505C and BHT-101 cells via immunofluorescence microscopy and ELISA. Similar to the Western blot analysis, miR-34b-5p restoration significantly reduced the expression level of Bcl-2, Notch1 and VEGF-A proteins in 8505C (**a**) and BHT-101 (**b**) cells when miR-34b-5p mimic transfected group, miR-1 transfected and scramble control groups were compared. Immunofluorescence images were captured by a Nikon A1R + confocal microscope using 60 × objective with immersion oil and Bcl-2, Notch1 and VEGF-A are stained red, and nuclei are stained blue; Scale in the immunofluorescent images shows 5 and 10 µm. In Western blotting, β-actin was used as a sample loading control. (8505C: anaplastic thyroid carcinoma from a papillary thyroid carcinoma origin; BHT-101: metastatic anaplastic thyroid carcinoma in lymph node). **c** Following transfection of K1, B-CPAP, 8505C, MB-1 and BHT-101thyroid carcinoma cells with miR-34b-5p mimic for 48 h, supernatants were collected for quantification of VEGF protein. ELISA assay data revealed that when compared to control cells, VEGF expression levels were inhibited in the supernatant fractions of thyroid carcinoma cells, transfected with miR-34b-5p. An asterisk indicates statistically significant differences ($p < 0.05$, Student's *t*-test) when compared to control cells

thyroid carcinoma) cell line transfected with miR-34b-5p (15 nM) mimic was also significantly increased by day 2 of transfection to 35.06% ± 18.33 with a significant drop in the S phase and G2-M phase compared with miR-1(15 nM) transfected and control groups (Fig. 5b) ($p < 0.05$). The introduction of miR-34b-5p (15 nM) mimic into the 8505C cell line (anaplastic thyroid carcinoma from a lymph node with primary papillary thyroid carcinoma) displayed its anti-growth abilities with a significant accumulation of cells in the G0-G1 phase (20.1% ± 9.12). There was also a significant drop in the S phase and G2-M phase, compared with miR-1(15 nM)

transfected and control groups ($p < 0.05$) (Fig. 5c). Anaplastic thyroid carcinoma cells (MB-1 and BHT-101) showed a similar trend with significant arrest in the G0-G1 of $20.53\% \pm 8.74$ and $23.83\% \pm 11.37$, respectively, followed by a significant drop in the S phase and G2/M phase ($p < 0.05$) (Fig. 5d, e). Collectively, a significant increase in the G0-G1 phase along with a reduction of cells in the G2-M phase were noted in the five different types of

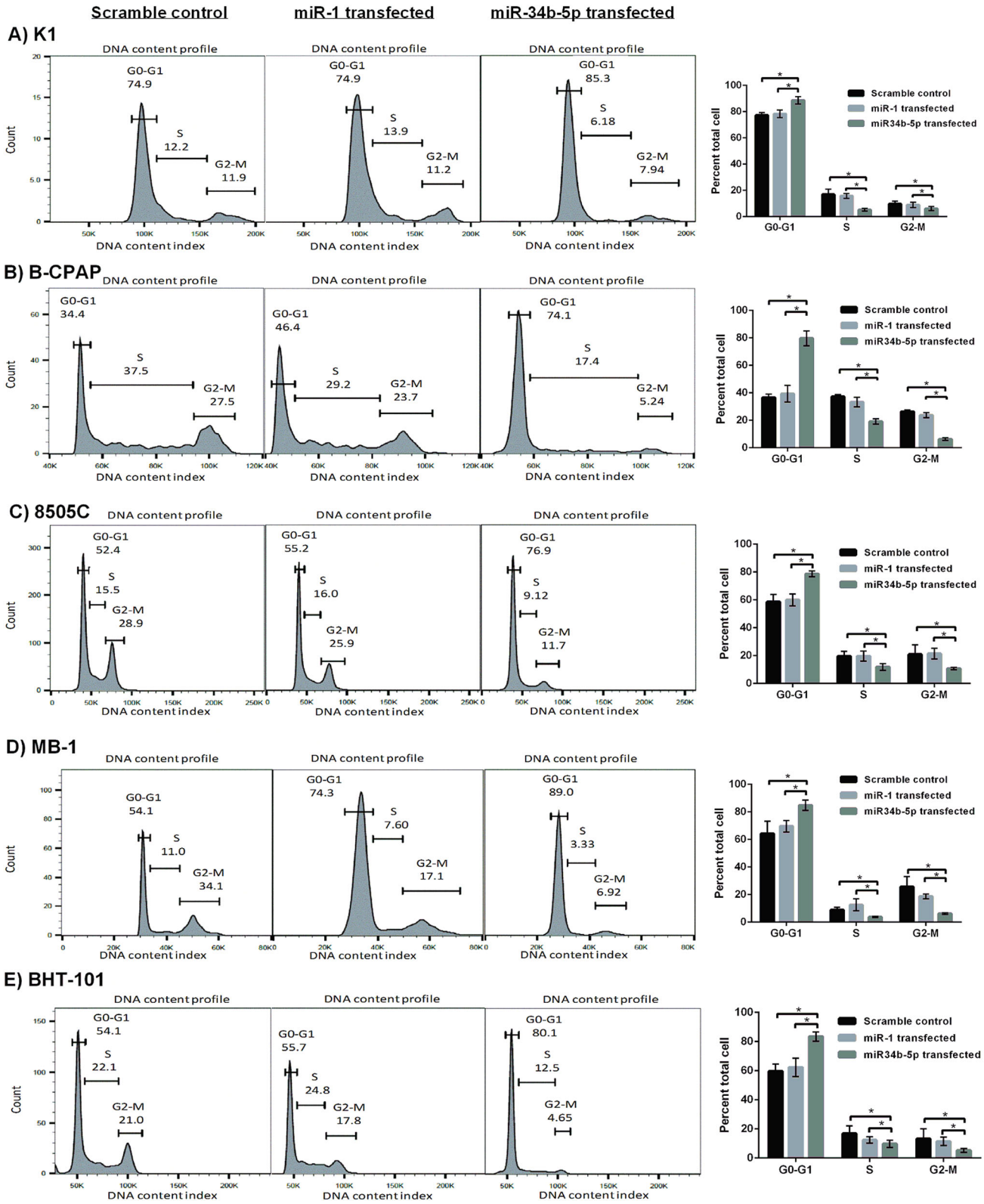

◀ **Fig. 5** miR-34b-5p induces the cell cycle arrest in thyroid carcinoma cell lines. Following transfection of **a**) K1, **b**) B-CPAP, **c**) 8505C, **d**) MB-1 and **e**) BHT-101 thyroid carcinoma cells with miR-34b-5p mimic or miR-1 for 48 h, nuclei of the carcinoma cells were stained with propidium iodide (PI) solution and analysed for DNA content by flow cytometry. Data were shown as mean ± SD of three independent experiments and represent percentage cells in different phases of the cell cycle with miR-34b-5p related to miR-1 and scramble treatments. Flow cytometry results indicated the cell number increased in G0-G1 phase and decreased in S phase when compared with miR-1 transfected and control groups. An asterisk indicates statistically significant differences ($p < 0.05$, Student's *t*-test) when compared to control cells (K1: papillary thyroid carcinoma; B-CPAP: metastatic papillary thyroid carcinoma in a lymph node; 8505C: anaplastic thyroid carcinoma from a papillary thyroid carcinoma origin; MB-1: anaplastic thyroid carcinoma; BHT-101: metastatic anaplastic thyroid carcinoma in a lymph node)

thyroid carcinoma cells when compared to miR-1 (15 nM) and control groups.

Expression of miR-34b-5p leads to increased cell death in thyroid cancer cells

Inhibition of growth of cell could be resulted from apoptosis induced by overexpression of miR-34b-5p. Herein, we further investigated the miR-34b-5p induced apoptotic changes of thyroid cancer cells. The increase in the G0-G1 phase induced by miR-34b-5p mimic suggests that high expression of miR-34b-5p can lead to the induction of cell death (Fig. 6). A few late apoptotic cells were observed in the control group. The early apoptotic rate in thyroid carcinoma cells treated with miR-34b-5p mimic was significantly different from the control group. However, in the miR-34b-5p-treated group, a large number of apoptotic cells was found (Fig. 6) ($p < 0.05$).

The early and late apoptosis rates of K1 (primary papillary thyroid carcinoma) transfected with miR-34b-5p mimic (15 nM) was significantly increased after 2 days of transfection (9.56% ± 5.14) when compared with transfected with miR-1 (15 nM) and the control groups (Fig. 6a) ($p < 0.05$).

The percentage of early and late apoptosis events were slightly increased in the B-CPAP cells (metastasizing papillary thyroid carcinoma) after 2 days of transfection with miR-34b-5p mimic, compared with mock transfected and scramble controls (2.69% ± 1.46) (Fig. 6b). Similar trends were also detected in the 8505C cells (metastatic anaplastic thyroid carcinomas from a lymph node with primary papillary thyroid carcinoma) with a slight increase in early and late apoptosis events after 2 days of transfection when compared to the mock and scramble control transfected (1.42% ± 0.69) (Fig. 6c). In anaplastic thyroid carcinoma (MB-1 and BHT-101), the early and late apoptotic features were also noticed to be increased significantly up to (6% ± 3.91) and (4.99% ± 3.31) respectively (Fig. 6d, e) ($p < 0.05$).

Discussion

In the present study, we have demonstrated the biological effects and tumour suppressive effects of miR-34b-5p for the first time in thyroid cancer tissues and cell lines. Altered expression levels of miR-34b-5p and its correlation with pathological T-stage in patients with thyroid carcinoma imply its potential regulatory effects in the initiation and progression of thyroid carcinoma. Our results are in agreement with finding by others in thyroid cancer tissue [21, 31, 32]. In addition, this study has noted multiple cellular effects of miR-34b-5p by modulating its downstream targets such as Bcl-2 and Notch1 proteins. Thus, it can be hypothesised that miR-34b-5p suppresses the tumour growth through this downstream effect in thyroid carcinomas.

Overexpression of VEGF-A often noted in tissues from patients with thyroid carcinoma and this overexpression correlated with the pathogenesis of thyroid carcinoma [12, 33]. In the current study, VEGF-A protein expression decreased significantly following miR-34b-5p overexpression. Thus, deregulation of miR-34b-5p has a potent effect on tumour growth and progression by regulating angiogenesis in thyroid carcinoma cells. Further functional assays, as well as in-vivo studies, are required to confirm miR-34b-5p's angiogenic regulation in thyroid carcinomas.

We noted pro-apoptotic and anti-proliferative effect for miR-34b-5p in cells from the five thyroid carcinoma cell lines, which is in agreement with previous studies on miR-34b in other cancers [19, 34, 35]. Previous studies have also pointed out the similar roles for miR-34a and miR-34b, particularly in the suppression of cancer cell cycle, mainly by induction of G0-G1 cell cycle arrest [19, 36–38]. In this study, miR-34b-5p induced cell cycle arrest at G0-G1 in thyroid carcinoma cells. The suppression of cell cycle was more pronounced in the cells from more aggressive type of thyroid carcinomas. These results imply the potential regulatory roles of miR-34b-5p in cancer cell growth and proliferation by targeting various checkpoints in the cell cycle.

Notch1 is a downstream target for miR-34b [20]. In addition, Notch signalling directly or indirectly implicated in the regulation of genes involved in angiogenesis such as VEGF-A [39]. Geers et al. found that papillary thyroid carcinoma had a higher number of Notch1- positive cells in comparison to normal or nodular hyperplastic thyroid [40]. Dysregulation of Notch1 prevents differentiation and results in inhibition of apoptosis, suggesting a potential oncogenic

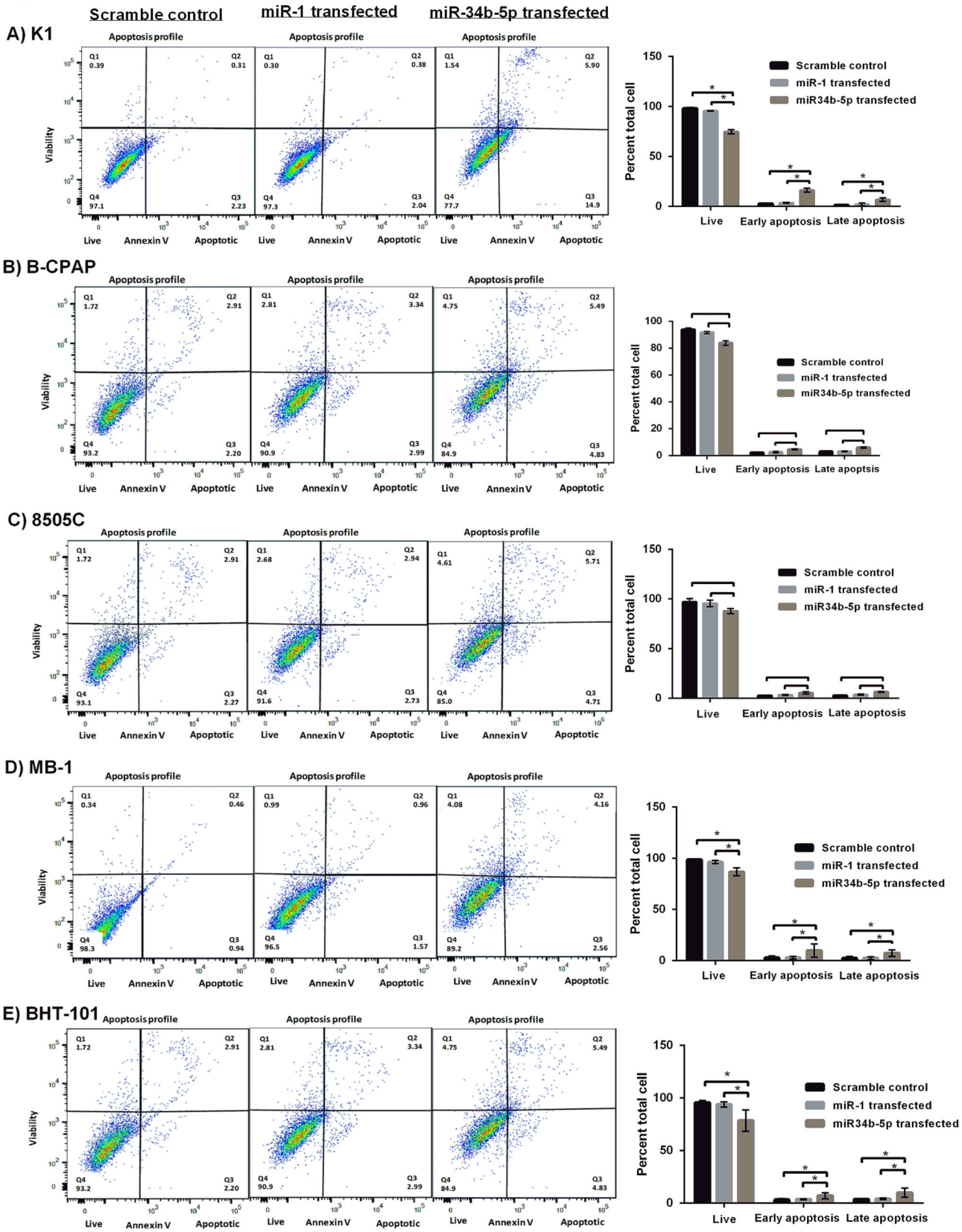
Scramble control
miR-1 transfected
miR-34b-5p transfected
A) K1
B) B-CPAP
C) 8505C
D) MB-1
E) BHT-101
Apoptosis profile
Viability
Annexin V
Live
Apoptotic
Percent total cell
Scramble control
miR-1 transfected
miR34b-5p transfected
Early apoptosis
Late apoptosis

◀ **Fig. 6** Re-expression of miR-34b-5p enhances apoptosis in thyroid carcinoma cell lines. Thyroid carcinoma cells transfected with either miR-34b-5p or miR-1 and scramble miRNA for 48 h. After 48 h, cells were subjected to Annexin V/propidium iodide (PI) staining and flow cytometry analysis. Data were shown as mean ± SD of three independent experiments. The data represented percentage of AnnexinV-positive cells with miR-34b-5p related to treatment (miR-1) and scramble control groups. The percentage of dead cells (Q1; upper left quadrant), live cells (Q4; lower left quadrant), late apoptosis cells (Q2; PI + /Annexin V + ; upper right quadrant) and early apoptosis cells (Q3; PI-/Annexin V + ; lower right quadrant) were indicated. Asterisks indicate statistically significant differences (* $p < 0.05$, Student's t-test) when compared to control cells ((**a**) K1: papillary thyroid carcinoma; (**b**) B-CPAP: metastatic papillary thyroid carcinoma in a lymph node; (**c**) 8505C: anaplastic thyroid carcinoma from a papillary thyroid carcinoma origin; (**d**) MB-1: anaplastic thyroid carcinoma; (**e**) BHT-101: metastatic anaplastic thyroid carcinoma in a lymph node)

role of Notch1 [40–42]. Similarly, this study has noted a significant downregulation of Notch1 protein expression in response to miR-34b-5p overexpression in thyroid carcinoma cells. Thus, Notch1 could be a potential mediator of miR-34b-5p's cellular effects in thyroid carcinoma.

In different cancers, enhancement of Bcl-2 expression increases the VEGF expression [43–45]. VEGF could also act as a survival factor for tumour cells by inducing the Bcl-2 expression and inhibiting apoptosis [46]. In addition, a study on prostate carcinoma revealed that Bcl-2 could interact with other factor (s) to regulate VEGF expression [43]. Notably, there was no involvement of these factors in the modulatory role of Bcl-2 in angiogenesis. Indeed, they found an exact similar expression level of transforming growth factor β−1 (TGFβ-1) and hypoxia-induced basic fibroblast growth factor (bFGF) in Bcl-2 transfected and untransfected groups [43, 47, 48]. This observation suggests that the effects of Bcl-2 on the VEGF expression level can be relatively specific.

In concurring with these observations, our results showed similar regulatory effects of miR-34b-5p on Bcl-2 and VEGF-A proteins, suggesting its potential role in the pathogenesis of thyroid carcinoma cells by modulating these genetic pathways. The current results indicated that miR-34b-5p induces cell death in thyroid carcinoma cells. This could be related to miR-34b-5p induced G0-G1 cell cycle arrest directly or due to suppression of Bcl-2 protein as a pro-survival factor [23, 49] or VEGF-A [24].

Regulation of Notch1 signalling pathways, as well as downstream effects on Bcl-2 and VEGF-A further, attributes to the mechanism behind miR-34b-5p induced cell cycle, apoptotic and angiogenic changes in thyroid carcinoma cells. As miR-34b-5p increases cell death in different carcinomas, miR-34b-5p induced apoptotic changes might be a common event in the pathogenesis of cancer [50–52]. Thus, our results further confirm the tumour suppressor role for miR-34b-5p in thyroid carcinomas.

In conclusion, this study indicates that miR-34b-5p downregulation may play a key role in the pathogenesis of the growth and proliferation of thyroid carcinoma. In addition, restoration of miR-34b-5p in thyroid carcinoma cells inhibited the expression of Bcl-2, VEGF-A and Notch1 proteins suggesting its target affinity towards these key regulators in molecular carcinogenesis. Furthermore, miR-34b-5p potentially functions through modulation of its downstream targets - Bcl-2, VEGF-A and Notch1. Thus, miR-34b-5p could be a target in the development of novel molecular therapeutic targets for metastatic thyroid carcinoma.

Acknowledgements We would like to thank the staff of Menzies Health Institute of Queensland and Dr Jelana Vider for their help in the laboratory work.

Funding The authors would like to thank the funding support of student scholarships from Griffith University, grant from Queensland Cancer Council and the project grants of the Menzies Health Institute of Queensland, Griffith University.

Ethical approval All experiments performed in this study involving human samples were in accordance with the ethical standards of Griffith University (MED/19/08/HREC) and with the 1964 Helsinki declaration and its later amendments or comparable to the ethical standards.

Compliance with ethical standards

Conflict of interest The authors declare that they have no competing interests.

References

1. A.K. Lam, C.Y. Lo, K.S. Lam, Papillary carcinoma of thyroid: a 30-yr clinicopathological review of the histological variants. Endocr. Pathol. **16**, 323–330 (2005)
2. K.Y. Lam, C.Y. Lo, K.W. Chan, K.Y. Wan, Insular and anaplastic carcinoma of the thyroid: a 45-year comparative study at a single institution and a review of the significance of p53 and p21. Ann. Surg. **231**, 329–338 (2000)
3. J. Weekes, Y.H. Ho, S. Sebesan, K. Ong, A.K. Lam, Irinotecan and colorectal cancer: the role of p53, VEGF-C and alpha-B-crystallin expression. Int. J. Colorectal. Dis. **25**, 907 (2010)
4. W.W. Xu, B. Li, A.K. Lam, S.W. Tsao, S.Y. Law, K.W. Chan, Q. J. Yuan, A.L. Cheung, Targeting VEGFR1- and VEGFR2-expressing non-tumor cells is essential for esophageal cancer therapy. Oncotarget **6**, 1790–1805 (2015)
5. X.M. Yu, C.Y. Lo, W.F. Chan, K.Y. Lam, P. Leung, J.M. Luk, Increased expression of vascular endothelial growth factor C in papillary thyroid carcinoma correlates with cervical lymph node metastases. Clin. Cancer Res. **11**, 8063–8069 (2005)
6. X.M. Yu, C.Y. Lo, A.K. Lam, B.H. Lang, P. Leung, J.M. Luk, The potential clinical relevance of serum vascular endothelial growth factor (VEGF) and VEGF-C in recurrent papillary thyroid carcinoma. Surgery **144**, 934–940 (2008)
7. X.M. Yu, C.Y. Lo, A.K. Lam, P. Leung, J.M. Luk, Serum vascular endothelial growth factor C correlates with lymph node metastases and high-risk tumor profiles in papillary thyroid carcinoma. Ann. Surg. **247**, 483–489 (2008)

8. A. Caporali, C. Emanueli, MicroRNA regulation in angiogenesis. Vascul. Pharmacol. **55**, 79–86 (2011)
9. J. Folkman, Angiogenesis in cancer, vascular, rheumatoid and other disease. Nat. Med. **1**, 27–30 (1995)
10. M. Meyer, M. Clauss, A. Lepple-Wienhues, J. Waltenberger, H.G. Augustin, M. Ziche, C. Lanz, M. Buttner, C. Dehio, A novel vascular endothelial growth factor encoded by Orf virus, VEGF-E, mediates angiogenesis via signalling through VEGFR-2 (KDR) but not VEGFR-1 (Flt-1) receptor tyrosine kinases. EMBO J. **18**, 363–374 (1999)
11. I. Stalmans, D. Lambrechts, F. De Smet, S. Jansen, J. Wang, S. Maity, P. Kneer, M. von der Ohe, A. Swillen, C. Maes, M. Gewillig, D.G. Molin, P. Hellings, T. Boetel, M. Haardt, V. Compernolle, M. Dewerchin, S. Plaisance, R. Vlietinck, B. Emanuel, A.C. Gittenberger-de Groot, P. Scambler, B. Morrow, D.A. Driscol, L. Moons, C.V. Esguerra, G. Carmeliet, A. Behn-Krappa, K. Devriendt, D. Collen, S.J. Conway, P. Carmeliet, VEGF: a modifier of the del22q11 (DiGeorge) syndrome? Nat. Med. **9**, 173–182 (2003)
12. A. Salajegheh, H. Vosgha, M.A. Rahman, M. Amin, R.A. Smith, A.K. Lam, Interactive role of miR-126 on VEGF-A and progression of papillary and undifferentiated thyroid carcinoma. Hum. Pathol. **51**, 75–85 (2016)
13. D.G. Duda, T.T. Batchelor, C.G. Willett, R.K. Jain, VEGF-targeted cancer therapy strategies: current progress, hurdles and future prospects. Trends Mol. Med. **13**, 223–230 (2007)
14. O. Casanovas, D.J. Hicklin, G. Bergers, D. Hanahan, Drug resistance by evasion of antiangiogenic targeting of VEGF signaling in late-stage pancreatic islet tumors. Cancer Cell **8**, 299–309 (2005)
15. P.T. Finger, K.J. Chin, E.A. Semenova, Intravitreal anti-VEGF therapy for macular radiation retinopathy: a 10-year study. Eur. J. Ophthalmol. **26**, 60–66 (2016)
16. P.T. Finger, S.K. Mukkamala, Intravitreal anti-VEGF bevacizumab (Avastin) for external beam related radiation retinopathy. Eur. J. Ophthalmol. **21**, 446–451 (2011)
17. L.C. Harshman, W. Xie, G.A. Bjarnason, J.J. Knox, M. MacKenzie, L. Wood, S. Srinivas, U.N. Vaishampayan, M.H. Tan, S.Y. Rha, F. Donskov, N. Agarwal, C. Kollmannsberger, S. North, B.I. Rini, D.Y. Heng, T.K. Choueiri, Conditional survival of patients with metastatic renal-cell carcinoma treated with VEGF-targeted therapy: a population-based study. Lancet Oncol. **13**, 927–935 (2012)
18. G. Lupo, N. Caporarello, M. Olivieri, M. Cristaldi, C. Motta, V. Bramanti, R. Avola, M. Salmeri, F. Nicoletti, C.D. Anfuso, Anti-angiogenic therapy in cancer: Downsides and new pivots for precision medicine. Front. Pharmacol. **7**, 519 (2016)
19. H. Maroof, A. Salajegheh, R.A. Smith, A.K. Lam, MicroRNA-34 family, mechanisms of action in cancer: a review. Curr. Cancer Drug Targets **14**, 737–751 (2014)
20. H. Maroof, A. Salajegheh, R.A. Smith, A.K. Lam, Role of microRNA-34 family in cancer with particular reference to cancer angiogenesis. Exp. Mol. Pathol. **97**, 298–304 (2014)
21. L. Yip, L. Kelly, Y. Shuai, M.J. Armstrong, Y.E. Nikiforov, S.E. Carty, M.N. Nikiforova, MicroRNA signature distinguishes the degree of aggressiveness of papillary thyroid carcinoma. Ann. Surg. Oncol. **18**, 2035–2041 (2011)
22. B.C. Bernardo, X.M. Gao, C.E. Winbanks, E.J. Boey, Y.K. Tham, H. Kiriazis, P. Gregorevic, S. Obad, S. Kauppinens, X.J. Du, R.C. Lin, J.R. McMullen, Therapeutic inhibition of the miR-34 family attenuates pathological cardiac remodeling and improves heart function. Proc. Natl. Acad. Sci. USA **109**, 17615–17620 (2012)
23. Q. Ji, X. Hao, Y. Meng, M. Zhang, J. DeSano, D. Fan, L. Xu, Restoration of tumor suppressor miR-34 inhibits human p53-mutant gastric cancer tumorspheres. BMC Cancer **8**, 266 (2008)
24. X.P. Li, W. Jing, J.J. Sun, Z.Y. Liu, J.T. Zhang, W. Sun, W. Zhu, Y.Z. Fan, A potential small-molecule synthetic antilymphangiogenic agent norcantharidin inhibits tumor growth and lymphangiogenesis of human colonic adenocarcinomas through blocking VEGF-A,-C,-D/VEGFR-2,-3 "multi-points priming" mechanisms in vitro and in vivo. BMC Cancer **15**, 527 (2015)
25. L. Liu, L. Liu, J. Shi, M. Tan, J. Xiong, X. Li, Q. Hu, Z. Yi, D. Mao, MicroRNA-34b mediates hippocampal astrocyte apoptosis in a rat model of recurrent seizures. BMC Neurosci **17**, 56 (2016)
26. W. Ye, Q. Lv, C.K. Wong, S. Hu, C. Fu, Z. Hua, G. Cai, G. Li, B. B. Yang, Y. Zhang, The effect of central loops in miRNA:MRE duplexes on the efficiency of miRNA-mediated gene regulation. PLoS One **3**, e1719 (2008)
27. F. Islam, V. Gopalan, S. Law, J.C. Tang, K.W. Chan, A.K. Lam, MiR-498 in esophageal squamous cell carcinoma: clinicopathological impacts and functional interactions. Hum. Pathol. **62**, 141–151 (2017)
28. V. Gopalan, F. Islam, S. Pillai, J.C. Tang, D.K. Tong, S. Law, K. W. Chan, A.K. Lam, Overexpression of microRNA-1288 in oesophageal squamous cell carcinoma. Exp. Cell Res. **348**, 146–154 (2016)
29. F. Islam, V. Gopalan, J. Vider, R. Wahab, F. Ebrahimi, C.T. Lu, K. Kasem, A.K.Y. Lam, MicroRNA-186-5p overexpression modulates colon cancer growth by repressing the expression of the FAM134B tumour inhibitor. Exp. Cell Res. **357**, 260–270 (2017)
30. F. Islam, V. Gopalan, R. Wahab, R.A. Smith, B. Qiao, A.K. Lam, Stage dependent expression and tumor suppressive function of FAM134B (JK1) in colon cancer. Mol. Carcinog. **56**, 238–249 (2017)
31. Y. Huang, D. Liao, L. Pan, R. Ye, X. Li, S. Wang, C. Ye, L. Chen, Expressions of miRNAs in papillary thyroid carcinoma and their associations with the BRAFV600E mutation. Eur. J. Endocrinol. **168**, 675–681 (2013)
32. X. Li, Z. Wang, The role of noncoding RNA in thyroid cancer. Gland Surg. **1**, 146–150 (2012)
33. A. Salajegheh, S. Pakneshan, A. Rahman, E. Dolan-Evans, S. Zhang, E. Kwong, V. Gopalan, C.Y. Lo, R.A. Smith, A.K.Y. Lam, Co-regulatory potential of vascular endothelial growth factor–A and vascular endothelial growth factor–C in thyroid carcinoma. Hum. Pathol. **44**, 2204–2212 (2013)
34. J. Xiao, Y. Li, W. Zhang, Y. Jiang, B. Du, Y. Tan, miR-34b inhibits nasopharyngeal carcinoma cell proliferation by targeting ubiquitin-specific peptidase 22. Onco Targets Ther. **9**, 1525–1534 (2016)
35. Y. Xie, P. Zong, W. Wang, D. Liu, B. Li, Y. Wang, J. Hu, Y. Ren, Y. Qi, X. Cu, Y. Chen, C. Liy, F. Li, Hypermethylation of potential tumor suppressor miR-34b/c is correlated with late clinical stage in patients with soft tissue sarcomas. Exp. Mol. Pathol. **98**, 446–454 (2015)
36. D.C. Corney, A. Flesken-Nikitin, A.K. Godwin, W. Wang, A.Y. Nikitin, MicroRNA-34b and MicroRNA-34c are targets of p53 and cooperate in control of cell proliferation and adhesion-independent growth. Cancer Res. **67**, 8433–8438 (2007)
37. L.G. Wang, Y. Ni, B.H. Su, X.R. Mu, H.C. Shen, J.J. Du, MicroRNA-34b functions as a tumor suppressor and acts as a nodal point in the feedback loop with Met. Int. J. Oncol. **42**, 957–962 (2013)
38. K.Y. Wong, R.L. Yim, C.C. So, D.Y. Jin, R. Liang, C.S. Chim, Epigenetic inactivation of the MIR34B/C in multiple myeloma. Blood **118**, 5901–5904 (2011)
39. T. Kangsamaksin, I.W. Tattersall, J. Kitajewski, Notch functions in developmental and tumour angiogenesis by diverse mechanisms. Biochem. Soc. Trans. **42**, 1563–1568 (2014)
40. C. Geers, I.M. Colin, A.C. Gerard, Delta-like 4/Notch pathway is differentially regulated in benign and malignant thyroid tissues. Thyroid **21**, 1323–1330 (2011)

41. M. Kunnimalaiyaan, H. Chen, Tumor suppressor role of Notch-1 signaling in neuroendocrine tumors. Oncologist **12**, 535–542 (2007)
42. A.S. Yamashita, M.V. Geraldo, C.S. Fuziwara, M.A. Kulcsar, C. U. Friguglietti, R.B. da Costa, G.S. Baia, E.T. Kimura, Notch pathway is activated by MAPK signaling and influences papillary thyroid cancer proliferation. Transl. Oncol. **6**, 197–205 (2013)
43. A. Fernandez, T. Udagawa, C. Schwesinger, W. Beecken, E. Achilles-Gerte, T. McDonnell, R. D'Amato, Angiogenic potential of prostate carcinoma cells overexpressing bcl-2. J. Natl. Cancer Inst. **93**, 208–213 (2001)
44. T.J. McDonnell, P. Troncoso, S.M. Brisbay, C. Logothetis, L.W. Chung, J.T. Hsieh, S.M. Tu, M.L. Campbell, Expression of the protooncogene bcl-2 in the prostate and its association with emergence of androgen-independent prostate cancer. Cancer Res. **52**, 6940–6944 (1992)
45. A. Takaoka, M. Adachi, H. Okuda, S. Sato, A. Yawata, Y. Hinoda, S. Takayama, K. Imai, Anti-cell death activity promotes pulmonary metastasis of melanoma cells. Oncogene **14**, 2971–2977 (1997)
46. K. Kuramoto, T. Uesaka, A. Kimura, M. Kobayashi, H. Watanabe, O. Katoh, ZK7, a novel zinc finger gene, is induced by vascular endothelial growth factor and inhibits apoptotic death in hematopoietic cells. Cancer Res. **60**, 425–430 (2000)
47. A. Biroccio, D. Del Bufalo, M. Fanciulli, T. Bruno, G. Zupi, A. Floridi, bcl-2 inhibits mitochondrial metabolism and lonidamine-induced apoptosis in adriamycin-resistant MCF7 cells. Int. J. Cancer **82**, 125–130 (1999)
48. A. Iervolino, D. Trisciuoglio, D. Ribatti, A. Candiloro, A. Biroccio, G. Zupi, D. Del Bufalo, Bcl-2 overexpression in human melanoma cells increases angiogenesis through VEGF mRNA stabilization and HIF-1-mediated transcriptional activity. FASEB J. **16**, 1453–1455 (2002)
49. Q. Ji, X. Hao, M. Zhang, W. Tang, M. Yang, L. Li, D. Xiang, J.T. Desano, G.T. Bommer, D. Fan, E.R. Fearon, T.S. Lawrence, L. Xu, MicroRNA miR-34 inhibits human pancreatic cancer tumor-initiating cells. PLoS One **4**, e6816 (2009)
50. Z. Hagman, O. Larne, A. Edsjo, A. Bjartell, R.A. Ehrnstrom, D. Ulmert, H. Lilja, Y. Ceder, miR-34c is downregulated in prostate cancer and exerts tumor suppressive functions. Int. J. Cancer **127**, 2768–2776 (2010)
51. C. Welch, Y. Chen, R.L. Stallings, MicroRNA-34a functions as a potential tumor suppressor by inducing apoptosis in neuroblastoma cells. Oncogene **26**, 5017–5022 (2007)
52. Y. Zhou, R.H. Zhao, K.F. Tseng, K.P. Li, Z.G. Lu, Y. Liu, K. Han, Z.H. Gan, S.C. Lin, H.Y. Hu, D.L. Min, Sirolimus induces apoptosis and reverses multidrug resistance in human osteosarcoma cells in vitro via increasing microRNA-34b expression. Acta Pharmacol. Sin. **37**, 519–529 (2016)
53. D. Betel, A. Koppal, P. Agius, C. Sander, C. Leslie, Comprehensive modeling of microRNA targets predicts functional non-conserved and non-canonical sites. Genome Biol. **11**, R90 (2010)